Current Genetics
https://doi.org/10.1007/s00294-019-01017-2

ORIGINAL ARTICLE

Expression of *Fusarium pseudograminearum FpNPS9* in wheat plant and its function in pathogenicity

Ruijiao Kang[1,2] · Guannan Li[1] · Mengjuan Zhang[1] · Panpan Zhang[1] · Limin Wang[1] · Yinshan Zhang[1] · Linlin Chen[1] · Hongxia Yuan[1] · Shengli Ding[1] · Honglian Li[1]

Received: 20 March 2019 / Revised: 9 July 2019 / Accepted: 10 July 2019

Abstract

Fusarium pseudograminearum-induced crown rot causes significant reduction to wheat production worldwide. To date, efforts to develop effective resistance to this disease have been hampered by the quantitative nature of resistance trait and a lack of understanding of the molecular pathogenesis. Non-ribosomal peptides have important roles in development, pathogenicity, and toxins in many plant pathogens, while less is known in *F. pseudograminearum*. In this work, we studied the expression and function of a nonribosomal peptide gene *FpNPS9* in *F. pseudograminearum.* We determined the expression of *FpNPS9* which was significantly up regulated during the infection of wheat. A deletion mutant *Δfpnps9* produced in this study displayed a normal growth and conidiation phenotype, however, hyphae polar growth was obviously affected. Deoxynivalenol production in this mutant was significantly reduced and the infection of wheat coleoptiles and wheat spikelet was attenuated. The *Δfpnps9* showed serious defects on the extension of infectious hyphae in plant and inhibition of roots elongation compared with the wild type. The complementation assay using a FpNPS9-GFP fusion construct fully restored the defects of the mutant. GFP signal was detected in the germinating conidia and infectious hyphae in coleoptiles of the infected plants. Interestingly, the signal was not observed when it was grown on culture medium, suggesting that the expression of *FpNPS9* was regulated by an unknown host factor. This observation was supported by the result of qRT-PCR. In summary, we provided new knowledge on *FpNPS9* expression in *F. pseudograminearum* and its function in *F. pseudograminearum* pathogenicity in wheat.

Keyword Fusarium crown rot · *Fusarium pseudograminearum* · Nonribosomal peptide synthetase · Pathogenicity · Deoxynivalenol (DON) · *FpNPS9*

Introduction

Wheat is the second most important staple food crop after rice and is cultivated in diverse areas worldwide (Singh et al. 2016). Fusarium crown rot (FCR) of wheat, primarily caused by the complex of Fusarium species including *Fusarium culmorum* (*Fc*), *F. pseudograminearum* (*Fp*), and *F. graminearum* (*Fg*), is a serious disease of economic significance in wheat cropping regions of the world (Akinsanmi et al. 2006; Obanor and Chakraborty 2014). Among the three causal agents, *Fp* led to the greatest yield losses (Dyer et al. 2009). In Australia, and the Pacific Northwest of the USA, FCR caused up to 35% reduction in wheat grain yields or even more in its favorable condition or without control (Akinsanmi et al. 2004; Kazan and Gardiner 2018; Liu and Ogbonnaya 2015; Murray and Brennan 2009; Smiley et al. 2005). In 2012, we first reported that *Fp* is the pathogen

Communicated by M. Kupiec.

Electronic supplementary material The online version of this article (https://doi.org/10.1007/s00294-019-01017-2) contains supplementary material, which is available to authorized users.

✉ Honglian Li
honglianli@sina.com

Shengli Ding
shengliding@henau.edu.cn

[1] Collaborative Innovation Center of Henan Grain Crops/ National Key Laboratory of Wheat and Maize Crop Science, Henan Agricultural University, Zhengzhou 450002, China

[2] Xuchang Vocational Technical College, Xuchang 461000, China

Published online: 16 July 2019

of FCR in Henan province of China (Li et al. 2012). Our research indicated that the disease impact of *Fp* is more severe than *Fg* and other soil-borne pathogens and has become the predominant pathogen of FCR in the Huanghuai winter wheat region (He 2016; Zhou et al. 2019). Disease symptoms of *Fp* usually appear on roots, sub-crown internodes, coleoptiles, leaf sheaths, stem bases, and internodes with honey brown discoloration initially that later turns dark brown or black and causes whiteheads in mature wheat and barley (Malligan 2009; Li et al. 2012; Xu et al. 2015; Wang et al. 2017). The fungal hyphae infect the leaf sheaths of seedlings often through natural openings such as stomata. *Fusarium pseudograminearum* then occupies the leaf sheath tissue and crosses to the neighbor cells through appressoria-like infection structures, but the hyphae are not observed in vascular tissue (Knight and Sutherland 2011, 2013). Toxins also act as virulence factors during *Fp* colonization of wheat crown and grain (Obanor and Chakraborty 2014; Powell et al. 2017). In addition to toxins, *Fp* can produce a wide range of other bioactive secondary metabolites including the cytokinin-like compound fusatin, polyketides (PKs), and small nonribosomal peptides (NRPs), which contribute to virulence or symptom development (Sørensen et al. 2018).

Nonribosomal peptide synthetases (NPS) are large multifunctional protein complexes that catalyze the synthesis of many NRPs by nonribosomal ways in fungi. NRPs have important biological activities. Recent studies have shown that NPSs play an important role in the process of pathogenic fungi infection of plants. In tomato leaf mold, a NPS was required for the pathogen, *Cladosporium fulvum,* to establish a biotrophic relationship with the host (Collemare et al. 2014). In *Alternaria alternata*, an apple pathotype, which causes Alternaria blotch of susceptible apple cultivars, NPSs are associated with the production of virulence factors, HC and AM toxin (Johnson et al. 2000). *NPS6* produces fusarinine, which is involved in virulence, resistance to oxidative stress, and the synthesis of extracellular siderophores in *C. heterostrophus*, *C. miyabeanus,* and *Alternaria brassicicola* (Lee et al. 2005; Shinichi et al. 2006). In *Fusarium*, *NPS6* is associated with pathogenicity, and the deletion of *NPS6* in *Fg* induces decreased virulence (Oide et al. 2006). *NPS1*, *NPS2*, and *NPS6* have overlapping functions as siderophores affecting the pathogenicity of *Fg* with *NPS2* acting as an intercellular siderophore related to the formation of sexual development of *Fg,* while *NPS1* and *NPS6* are extracellular siderophores (Oide et al. 2007, 2014; Tobiasen et al. 2007). *NPS22* produces enniatin B and beauvericin in *F. oxysporum* (Hansen et al. 2015). In *F. solani*, *NPS30* produces sansalvamide, an anti-tumor material (Romans-Fuertes et al. 2016). *NPS4* can increase the hydrophobicity of cells in *Fg*, which may be related to cell wall synthesis (Hansen et al. 2012).

During plant infection, *NPS9* was specifically induced at 64 h after inoculation (HAI) in *Fg,* and *NPS9* cluster deleted mutants showed reduced virulence during coleoptile infection in *Fg* (Zhang et al. 2012). A linear nonribosomal fusaoctacin A, produced by *NPS9* and *NPS5*, contributes to wheat coleoptile invasion ability along with the suppression of host defense response (Jia et al. 2019). Our transcriptome data (unpublished) showed that an *FpNPS9* gene, the homologous gene of *NPS9* in *Fp*, upregulated during the infection of wheat roots and basal stems with *Fp*, but the function of *FpNPS9* was not known. Here, we applied split-marker strategy to delete *FpNPS9* and performed the functional characterization of the *FpNPS9* gene which required for the development, pathogenicity, and extension in wheat.

Materials and methods

Strain, wheat, and culture conditions

The wild type WZ-8A of *F. pseudograminearum* was isolated locally and preserved in our laboratory. The tested wheat varieties were Aikang58, Guomai301, and Zhoumai24. The fungal strains cultured in solid PDA (200 g diced and peeled potatoes were boiled for 20 min and filtered through four layers of cheesecloth; water was added with 20 g dextrose 15 g agar to filtrate to 1000 ml, then autoclaved at 121 °C for 30 min). The potato dextrose broth (PDB) was without agar, while potato sucrose (PS) with 20 g sucrose (replacement of dextrose). The Czapek medium (2 g $NaNO_3$, 0.5 g KCl, 0.01 g $FeSO_4$, 1 g K_2HPO_4, 0.5 g $MgSO_4$, 30 g sucrose, 20 g agar, and 1000 ml distilled water) without $FeSO_4$ and YEPD broth (1% yeast extract, 2% Bacto-peptone, and 2% dextrose) were used for fungal cultures prior to morphology comparison, toxin production, and quantitative RT-PCR (qRT-PCR) analysis. For the conidiation test, four pieces of 5 mm fungal agar dishes were put in a 50 ml flask containing 20 ml of CMC (2% solution of carboxymethyl cellulose) with shaking at 150 rpm at 25 °C (Wang et al. 2017). Sensitivity assays of WT strain, Δ*fpnps9-5* mutant and Δfpnps9-C strain to several abiotic stresses were performed on complete medium (CM) (Yang et al. 2018) with 1 M NaCl, 1 M KCl, 1 M Sorbitol, 0.05% SDS, 1 mg/ml Congo Red (CR), and 20 mM H_2O_2, respectively (Ding et al. 2018; Yang et al. 2018). The experiments were repeated three times.

Molecular analysis

Genomic DNA was isolated from mycelia, cultured in YEPD broth for 2–3 days and filtered with water rinsing, using the CTAB method (Leslie and Summerell 2006). Total RNA was extracted from conidia, hyphae, and infected wheat samples harvested at 1, 2, and 3 dpi using Trizol reagent (Ambion by Life Technologies 15596026) following the manufacturer's

instructions. The quality of RNA was assessed by agarose gel electrophoresis and measured using an ultramicro spectrophotometer (Thermo). cDNA was generated according to the instructions of the PrimeScript® RT reagent Kit (Perfect Real Time, TaKaRa Code: DRR047A) (Sun et al. 2015). The genomic DNA was digested by restriction endonuclease *Kpn* I and separated in an agarose gel. Hygromycin phosphate dehydrogenase (*HPH*) gene was used as a probe labeled with Roche's DIG High Prime DNA Labeling and Detection Kit Π.

Identification and expression of *FpNPS9*

Transcriptome sequencing was carried out using the roots and basal stems from seedlings of susceptible and resistant wheat cultivars, Guomai301 and Zhoumai24, in pots with millet inoculums. Fresh WZ-8A culture on PDA plate was inoculated in millet media in a flask, placed in a growth chamber for 4–5 days at 25 °C until the mycelia totally covered the millet, and dried for inoculation into pots. Wheat seeds were treated with 3% sodium hypochlorite for 3 min, rinsed with sterile water, and placed in a Petri dish at room temperature for 48 h until germination. The germinated seeds were then put in pots that contained a 200 g mixture of sterile soil and millet inoculums at a 3% (w/w) ratio. The pots with sterile soil and millet without fungal inoculum were used as a control. All treatments had three replicates. After 5 day (early stage of infection) and 15 day (middle and late stage of infection), the seedlings were pulled out and the roots were rinsed with tap water. The root and basal stem were cut and frozen in liquid nitrogen for RNA preparation. RNA-seq was conducted with an Illumina HiSeq™ 4000 by the Gene Denovo Biotechnology Co. (Guangzhou, China). The gene and ORF fragment of *FpNPS9* were cloned from genomic DNA and cDNA library of *Fp*, respectively. The protein functional domains were predicted via http://smart.embl-heidelberg.de/.

Quantitative RT-PCR was conducted with the SYBR® Premix Ex Taq™II system. The cDNA library was generated from total RNA extracted from the conidia, mycelia, and wheat coleoptiles at 18, 30, and 48 h, and 3, 5, and 7 day after infection. The qRT-PCR reaction system was 12 µl in total containing 6 µl of 2 × SYBR® Premix Ex Taq™II mixture (TaKaRa), 0.5 µl of 10 µM each primer, 1 µl of cDNA solution, and 4 µl of RNase-free water. The amplification program was as follows: 95 °C for 2 min, followed by 40 cycles at 95 °C for 30 s, and 58 °C for 30 s. The partial *FpNPS9* cNDA was amplified from the cDNA library as the template using the primer pairs *NPS9RT-F1/NPS9RT-R1*; TEF1α gene (FPSE_11980) was selected as an internal reference gene and amplified with the primer pair *TEF1α*-RTF/*TEF1α*-RTR.

Knockout of *FpNPS9* with PEG-mediated protoplast transformation in *F. pseudograminearum*

Protoplast preparation of *Fp* and gene deletion was based on the methods of Wang et al. (2017). Briefly, primers F1/R1 and F2/R2 were designed to amplify the upstream and downstream fragments of the target gene (T1 and T2) from genomic DNA, while the primers HYG-F/HY-R and YG-F/HYG-R were used for the 2/3 fragments H1 and H2 of the *HPH* gene from plasmid pKOV21 (Fig. 1a). The two fusion fragments of T1-H1 and H2-T2 were generated with primers F1/HY-R and YG-F/R2, respectively (Fig. 1b). All the primers and sequences are listed in Table 1. The mixed resulting fragments of T1H1 and H2T2 were used for PEG-mediated transformation of WZ-8A protoplast (Fig. 1c). The transformants with hygromycin resistance were first screened by PCR, Southern blot analysis and RT-PCR (Fig. 1d, e) (Wang et al. 2017). For whole genome resequencing, mycelia of three mutants were collected after cultured 3 day in flask with YEPD broth, and sent to Gene Denovo Biotechnology Co. High-quality Illumina reads from genomic DNA were mapped against the reference genome sequence of *F. pseudograminearum* (CS3096) (http://fungi.ensembl.org/Fusarium_pseudograminearum/Info/Index) and determinated where the *HPH* located in mutants genome.

Pathogenicity assay

Pathogenicity was assayed as described by Wang et al. (2017) with some modification. When coleoptiles grew to 2–3 cm in length, the apex was cut off about 2 mm and inoculated into a 2 µl conidial suspension of 1.0×10^7/ml in sterile H_2O. The water with no conidium was used as a control. Intact coleoptiles were wrapped in sterile microscope lens paper and 20 µl of the 1.0×10^6/ml conidial suspension in sterile H_2O was dripped on them. The treatments were kept at 25 °C in a moist chamber in the dark for 24 h, then subjected to cycles of 16 h illumination/8 h dark. The wheat coleoptiles were harvested at 18 h, 30 h, 48 h, 3 day, 5 day, and 7 day post inoculation (dpi) for the samples of gene expression analysis. Each treatment had three replicates. The incidence of disease was recorded at 4 dpi and the diseased coleoptiles were detached for fluorescent staining following Knight and Sutherland protocol (2011). During wheat flowering stage in the field, the tip of a spikelet was cut and 10 µl of 1.0×10^6/ml was dropped in the spikelet covering with paper bag to keep moisture for 72 h. The spikelet infection was investigated and photographed after 2 weeks.

To compare effects of surfactants, four different kinds of surfactants were tested and the conidia were resuspended at 1.0×10^6/ml in 0.05% Tween 20, silwet, carboxymethyl cellulose (CMC), sodium dodecyl benzene sulfonate (SDBS),

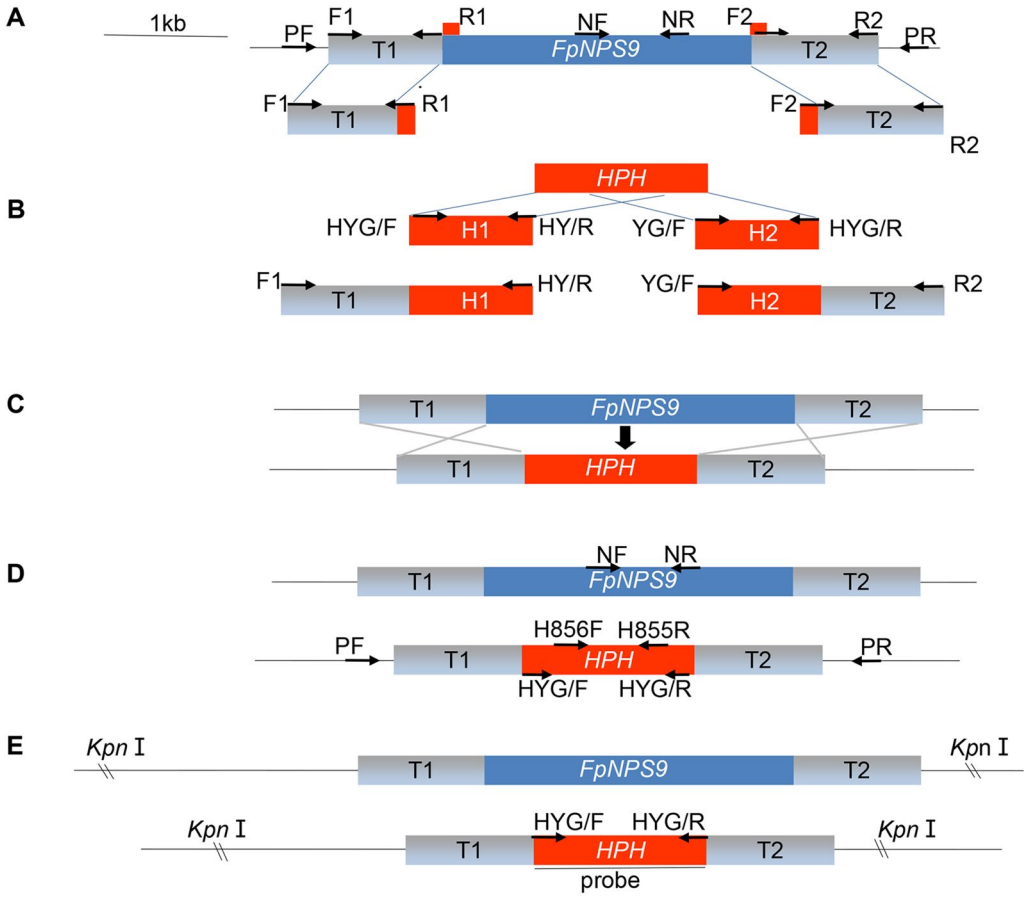

Fig. 1 Schematic diagram showing the process of gene deletion and diagnoses of deletion mutants. **a** DNA fragments upstream and downstream of the target gene were amplified with primer pairs F1/R1 and F2/R2. The R1 and F2 primers were designed to have tails that anneal to the selectable marker (*HPH*). The H1 and H2 fragments of the *HPH* gene were amplified with primer pairs HYG-F/HY-R and YG-F/HYG-R, respectively. **b** The upstream fragment T1 with H1 and H2 with downstream fragment T2 were fused together using primers F1 and HY/R and YG/F and R2, respectively, to generate two linear fragments (T1H1 and H2T2, respectively) for transformation. **c** Homologous recombination results in the replacement of the gene *FPNPS9* with the selectable marker (*HPH*). **d** Diagnostic PCR using four primer pairs PF/H855R, HYG-F/HYG-R, H856F/PR, and NF/NR results in distinguishable product size of WT (NF/NR, 656 bp) and transformants (PF/H855R, 1138 bp; HYG-F/HYG-R, 1380 bp; H856F/PR, 1326 bp). **e** Gene deletion mutant identified by Southern blot analysis. The restriction enzyme *Kpn* I was used for the digestion of genomic DNA and the full length *HPH* gene generated by the HYG/F and HYG/R primer pair was used as a probe

and sterile H_2O, respectively. The similar wrapped coleoptile inoculation as above was performed.

Complementation of the *Δfpnps9* deletion mutant

The *FpNPS9* gene, including a promoter region of about 2000 bp and a coding region without a stop codon cloned introduced with *Cla* I and *Apa* I restriction enzymes from WZ-8A genomic DNA, was inserted into the vector pKNTG cut with the same enzymes (*Cla* I and *Apa* I) and fused with the GFP gene. The resulting construct, pCfpnps9-GFP, was transformed into the protoplast of *Δfpnps9* mutant via PEG-mediation. The transformants with G418 resistance were screened using primer pairs Pfl2-gfp-F/Pfl2-gfp-R and Neo-F/Neo-R, and check the GFP fluorescent signal under Nikon microscope.

The expression of the GFP and Neo genes were, respectively, detected by two pairs of primers pKNTG-com-F/pKNTG-com-R and NPS9-cDNA-F1/NPS9-cDNA-R1 using RNA extracted from the infected wheat coleoptiles. pKNTG-com-F and pKNTG-com-R were located in the target gene and GFP gene, respectively, while primers NPS9-cDNA-F1 and NPS9-cDNA-R1 spanned exons in case of genomic DNA contamination of total RNA. The tubulin and actin genes were used as the references with the primers Fp-tublin-F/R and Fp-actin-F/R.

Table 1 Primers used in this study

Primers	PRIMER SEQUENCE 5′–3′
FP-NPS9-PF	GTATATCATCTTAGCCGAAACCCGTACTGG
FP-NPS9-F1	GTCCTCGCTAGAGACTCAAGATATGGAGAG
FP-NPS9-R1	TTGACCTCCACTAGCTCCAGCCAAGCCCTGCGTGGT ATAGCATGAAGTTGC
FP-NPS9-F2	ATAGAGTAGATGCCGACCGCGGGTTC CATTGAGGA GAATCCGTGCCTGTC
FP-NPS9-R2	CCTTCCAGTCTGTCGGTCTATGAGGCCATTGTTC
FP-NPS9-NF	CGGACCTAGAAGGTCAACAATGCCAG
FP-NPS9-NR	CATTGAGGAGAATCCGTGCCTGTC
FP-NPS9-PR	CCATAGATGGACAAGCATCCATGATCTCA
HYG-F	GGCTTGGCTGGAGCTAGTGGAGGTCAA
HY-R	AAGCCTGGCGTTCCTTAGCCAGTTATG
YG-F	GATGTAGGAGGGCGTGGATATGTCCT
HYG-R	TATCTCATCTACGGCTGGCGCCCAAG
TEF1a-RTF	TCACCACTGAAGTCAAGTCC
TEF1a-RTR	ACCAGCGACGTTACCACGTC
FpNPS9RT-F1	CTACTACCATCGGTCAGCTTCTCG
FpNPS9RT-R1	ATGAACGACCTAGAAGTGTGCGAA
NPS9IC-F	CCGGAATTCATGGCTCCTCTTAACACTTATACGTC
NPS9IC-R	CGCGGATCCTAAGACAGTAACTGTAACCTGGACATC
NPS9-cDNA-F1	GAGTTGCAAGATAAACGATGAACG
NPS9- cDNA-R1	ATGGCTCCTCTTAACACTTATACG
NPS9-com-Fb	TATGGGCCCGAGATGCTAGAAAAGGTCCTGAATG
NPS9-com-R	CCCATCGATTAAGACAGTAACTGTAACCTGGACA
pKNTG-com-F	TGAACACCAATTCAAAGCGG
pKNTG-com-R	CGTTGTGGCTGTTGTAGTTGT
Pfl2-gfp-f	CGTAAACGGCCACAAGTTCA
Pfl2-gfp-R	CTTGTACAGCTCGTCCATG
Neo-F	GGCCACAGTCGATGAATCCAGA
Neo-R	GAGAGGCTATTCGGCTATGACT
Fp-tubulin-F	GCCTTCACAACTCGCCATTG
Fp-tubulin-R	TTACGCATCGGTCTGAGTGG

Detection of mycotoxin deoxynivalenol (DON) in wheat

The wheat kernels were soaked in water for 10–15 h, boiled until there was no white inside and the epidermis was not broken, taken out and dried to the surface without water. Fifty grams of the wheat kernels was taken in a 250 ml flask and autoclaved at 121 °C for 2 h. Three plugs (5 mm diameter) were cut from the edge of 2- to 3-day colony of *F. pseudograminearium* wild-type WZ-8A and FPNPS9-5 mutant on PDA plates and transferred to the wheat kernels in flasks. The test and non-inoculated control (CK) were three replicates and the containers were kept in incubator at 25 °C with shaking vigorously by hand to break up the lumps every day. The kernel cultures were harvested at 30 dpi, dried in an oven at a temperature not exceeding 50°, and ground to a powder. Two grams powder passed through a 60-mesh sieve was sent for determination. After extraction by polyethylene glycol and purified by immunoaffinity column, DON was determined via High Performance Liquid Chromatography (HPLC).The results were analyzed according to the national standards of China (GB5009.111-2016).

Results

Identification of the NPS9 ortholog in *Fp*

Fusarium pseudograminearum genome annotation indicated that FPSE_02493 is the ortholog of NPS9 with a coding region of 2460 bp contains two exons encoding a non-ribosomal peptide synthetase with 819 amino acid residues. Smart BLAST search showed one conserved adenylate formation domain (A) and a thiolation domain (T) with one phosphopantetheine attachment site (Fig. 2a). Fp*NPS*9 is conserved in filamentous fungi with identities ranging from 36% to 97% in *Fusarium*,

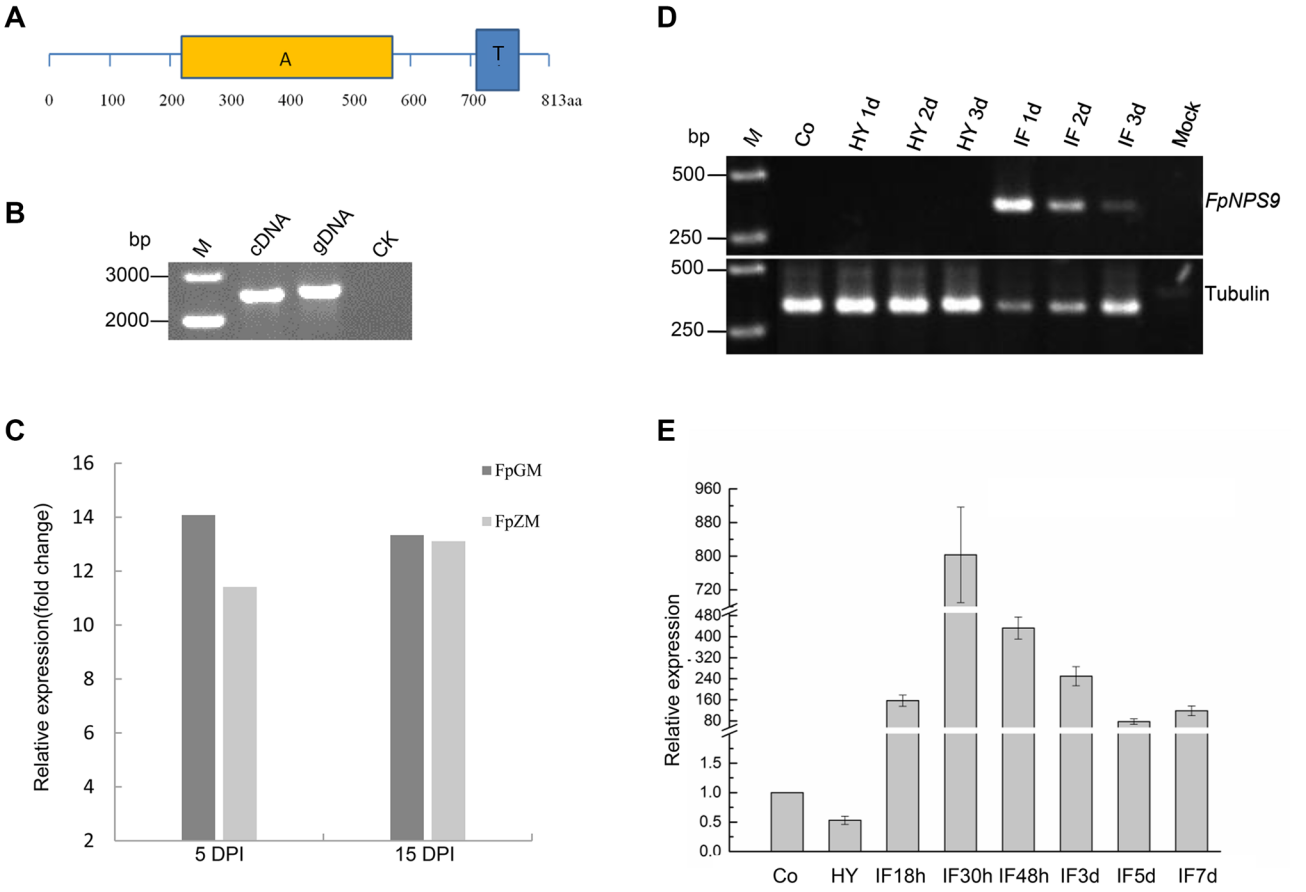

Fig. 2 Identification of the *FpNPS9* gene and expression profiles. **a** The diagram of *FpNPS9* contains the conserved A domain and T (or PCP) domain. **b** Agarose gel electrophoresis showed PCR products of full length *FpNPS9* ORF (2460 bp) and encoding region (2514 bp) from cDNA and genomic DNA, respectively, using primer pair NPS9IC-F/NPS9IC-R. gDNA, template of genomic DNA; cDNA, template of complement DNA from infected coleoptiles at 2 dpi; CK, ddH_2O.**c** Expression profiles of *FpNPS9* in the susceptible and resistant wheat cultivars. Fp-GM and Fp-ZM: the susceptible and resistant wheat varieties Guomai 301 and Zhoumai 24 were, respectively, inoculated with *Fp* strain WZ-8A; IF5 day and IF15 day: 5 day and 15 day post inoculation. **d** The RT-PCR products of *FpNPS9* from conidia, vegetative hyphae, and wheat coleoptiles in infection time courses were separated using an agarose gel. M: 2000 bp DNA marker; Co: conidia; HY1d, HY2d, HY3d: The culture of the hyphae in YEPD liquid medium after incubation for 1 day, 2 day, and 3 day, respectively. IF 1 day, IF 2 day, IF 3 day: 1 day, 2 day, and 3 day inoculated with *Fp*. Beta-tubulin was used as a reference gene. **e** The histogram of relative expression of *FpNPS9* in conidia, hyphae, and inoculation time course. *CO* conidia, *HY* hyphae; IF 18 h, IF 24 h IF 30 h IF 48 h, IF 3 day, IF 5 day, IF, 7 day: time course during wheat coleoptile inoculation with conidial suspensions

Colletotrichum, *Pyrenophora*, *Alternaria*, *Aspergillus*, and *Trichoderma* species.

To experimentally identify and clone the FPSE_02493 gene in our local strain, we prepared RNA from vegetative mycelia and wheat coleoptiles infected by *Fp* for 2 day. The ORF sequence of the *FpNPS9* gene was only amplified using cDNA of wheat coleoptile infection as a template. The resulting PCR product was consistent with the prediction that the transcript is 2460 bp (Fig. 2b).

Dynamic expression of *FpNPS9* during the time course of wheat infections

Due to undetectable *FpNPS9* transcript in the vegetative stage, we further investigated the dynamic expression of the *FpNPS9* gene in resistant and susceptible cultivars. At 5 and 15 dpi (days post inoculation), *FpNPS9* was relatively more upregulated in the susceptible cultivar Guomai

301 than that in the somewhat resistant cultivar Zhoumai 24, but the difference was not significant (Fig. 2c).

To fully investigate expression of *FpNPS9,* we extracted the total RNA from conidia from CMC media, vegetative mycelia cultured for 1, 2 and 3 day in YEPD media, and the infected wheat coleoptiles at 1, 2, and 3 dpi. PCR products were only amplified from cDNA of infected wheat coleoptiles with early induction at 1d, while no band was generated from cDNA of conidia and three mycelia samples (Fig. 2d).

We also conducted qRT-PCR to detect *FpNPS9* expression from conidia, mycelia, and coleoptiles at 18 h, 30 h, 48 h, 3 day, 5 day, and 7 day post inoculation. Expression of *FpNPS9* was low to undetectable in conidia and mycelia (Ct values of 30.90 and 30.35, respectively). The expression was significantly up-regulated during the infection stage by 156.91-fold, 803.10-fold, and 432.60-fold at 18 h, 30 h, and 48 h, respectively, while after 48 h, expression gradually decreased (Fig. 2e). The expression results demonstrated that *FpNPS9* is an infection-specific gene in secondary metabolism contributing to the infection of wheat.

Deletion of *FpNPS9* in *F. pseudograminearum* through homologous recombination

To characterize the biological function of *FpNPS9*, we deleted it in WZ-8A through homologous recombination. More than 50 candidate transformants with hygromycin resistance were obtained. After PCR screening with

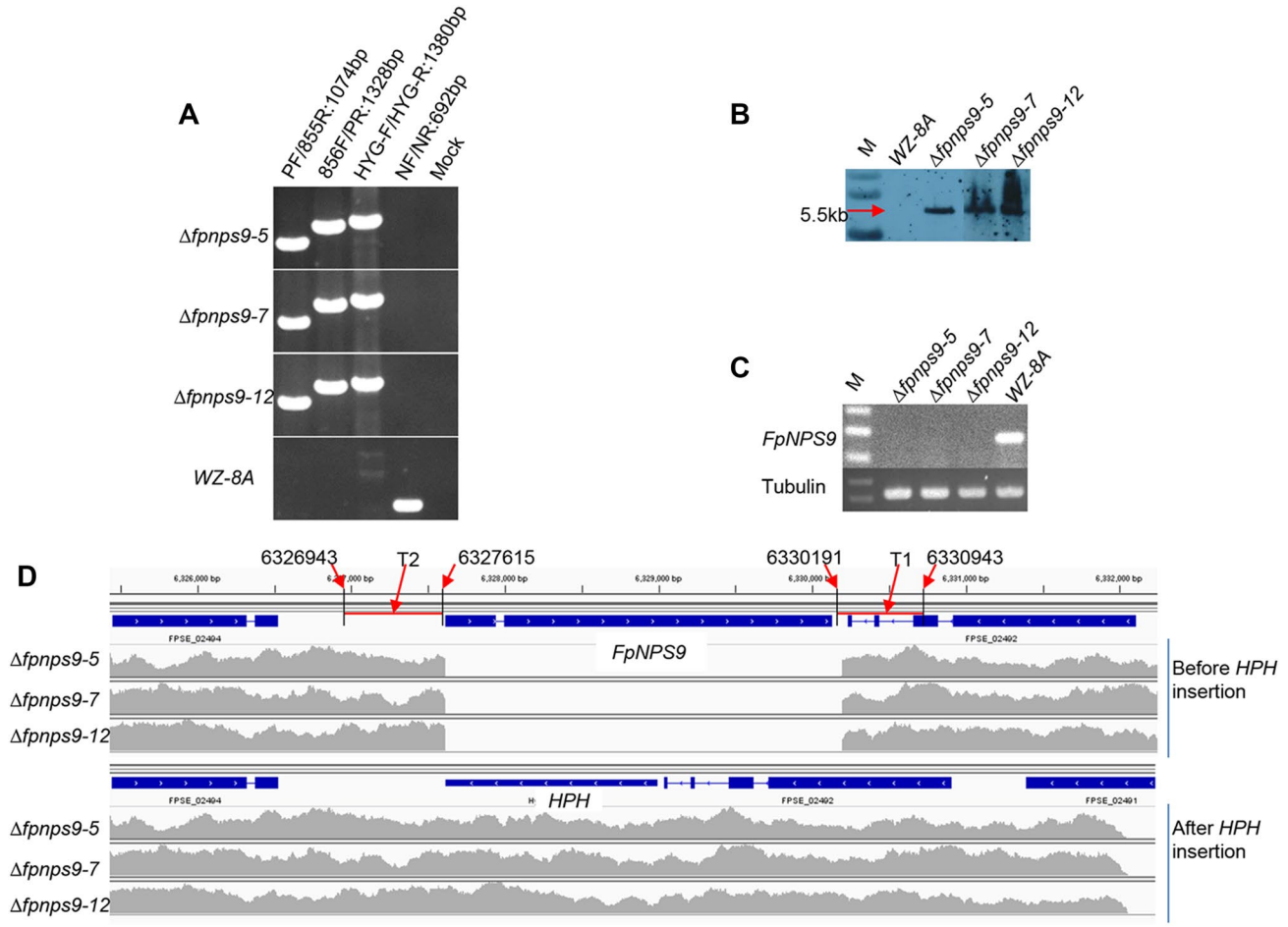

Fig. 3 Knockout of *FpNPS9* through homologous recombination. **a** The products of PCR screening for *Δfpnps9* deletion mutant by four primer pairs were separated in an agarose gel. *Δfpnps9-5*, *Δfpnps9-7*,*Δfpnps9-12*: *Δfpnps9* deletion mutants. WT, WZ-8A.**b** Southern blot confirmation of the *Δfpnps9* deletion mutant after autograph on film. The genomic DNA from *Δfpnps9*-5, *Δfpnps9-7*, *Δfpnps9-12*, and wild-type WZ-8A was digested by *Kpn* I and separated in an agarose gel. The full length of *HPH* gene was used as probe. The predicted single fragment in mutant with correct homologue replacement event was 5.5 kb in size. **c** Detection of *FpNPS9* expression in three mutants *Δfpnps9-5, Δfpnps9-7*, and *Δfpnps9-12* in comparison with wild type using cDNA of infected wheat coleoptiles as template with beta-tublin gene as reference. **d** IGV software clearly showed the three mutants with the FpNPS9 replacement by *HPH* gene after mapping the whole genome resequencing reads against the *F. pseudograminearum* reference genome. The red lines indicated the upstream and downstream of *FpNPS9* which was used for the homology recombination. The red arrows showed the location of the start and ends

four primer pairs to detect the negative, two positives, and hygromycin, and Southern blot analysis with *HPH* gene as probe, we got three Δ*fpnps9* mutants: *Δfpnps9-5*, *Δfpnps9-7*, and *Δfpnps9-12* (Fig. 3a, b). We further confirmed through RT-PCR and whole genome resequencing analysis. All three strains *Δfpnps9-5*, *Δfpnps9-7*, and *Δfpnps9-12* were clearly target gene deletion mutants (Fig. 3c, d).

Deletion mutant *Δfpnps9* does not affect hyphal growth, conidiation, iron metabolism

The morphology and growth rate of the three *Δfpnps9* mutants on PDA and -Fe Czapek medium and conidiation in CMC medium were similar to wild type (Fig. 4a, Table 2), even though the morphology of the hyphal tip looked abnormal under the microscope (Fig. 4b). This indicated that the *Δfpnps9* null mutant affect the growth of hyphal tip, but did

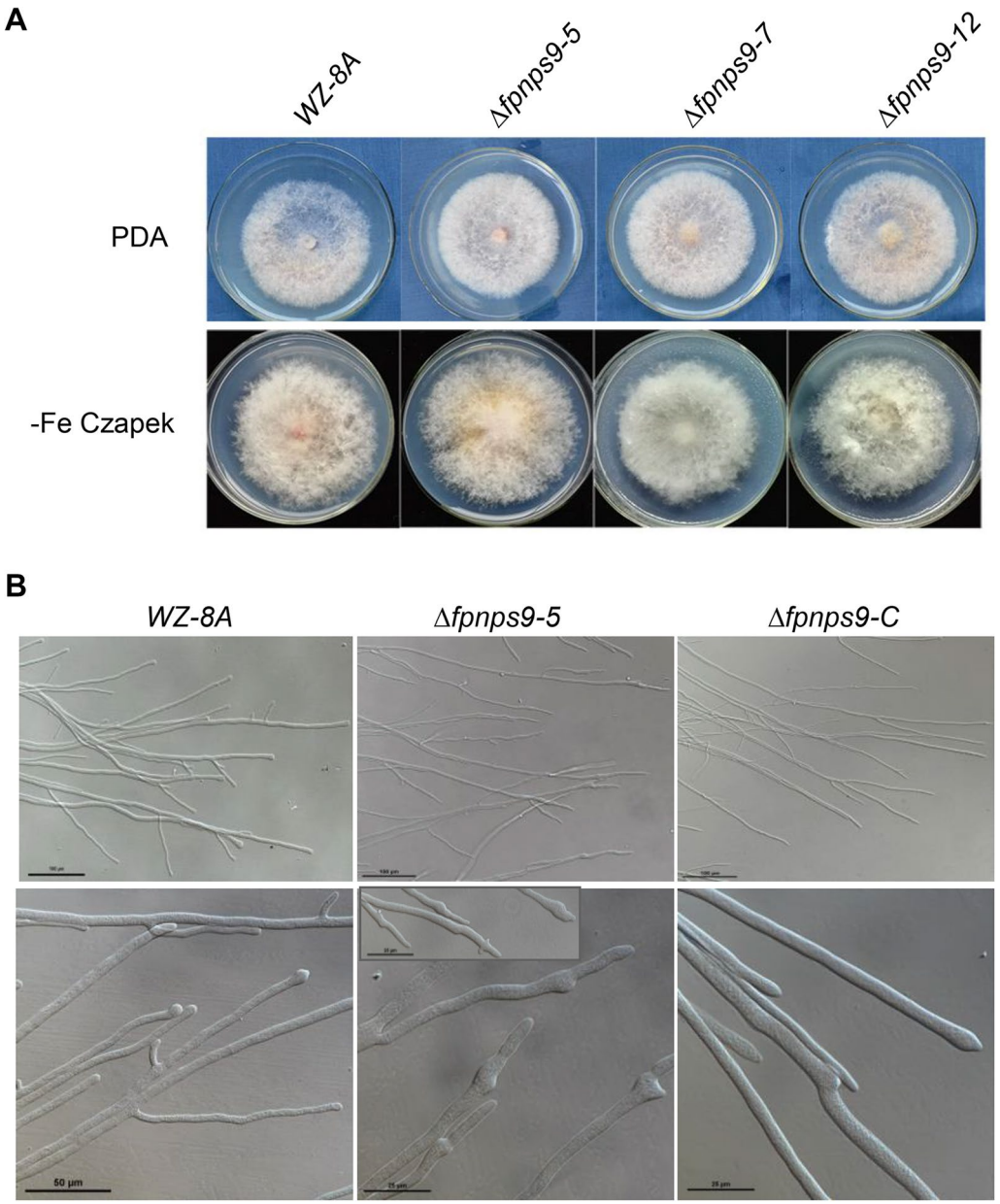

Fig. 4 Colony and hyphae tip morphologies. **a** Morphology of the *Δfpnps9* deletion mutant *Δfpnps9-5*, *Δfpnps9-7*, and *Δfpnps9-12* with wild-type on PDA plates and -Fe Czapek medium. **b** The abnormal hyphae polarization of the *Δfpnps9* deletion mutant in comparison to wild-type WZ-8A

Table 2 Phenotypes of the *FpNPS9* mutants in growth, conidiation, and DON production

Strains	Growth on PDA (cm)	Czapek-Fe (cm)	Condition ($\times 10^6$)	DON ($\times 10^3$ μg/kg kernels)
WT	6.48 ± 0.42	6.43 ± 0.28	4.83 ± 0.88	7.47 ± 0.46
Δfpnps9-5	6.80 ± 0.59	6.66 ± 0.60	3.75 ± 1.64	4.85 ± 0.45*
Δfpnps9-7	6.77 ± 0.66	6.90 ± 0.43	3.50 ± 1.73	/
Δfpnps9-12	6.20 ± 1.68	7.14 ± 0.30	3.19 ± 1.66	/
Δfpnps9-C	/	/	/	6.36 ± 0.25

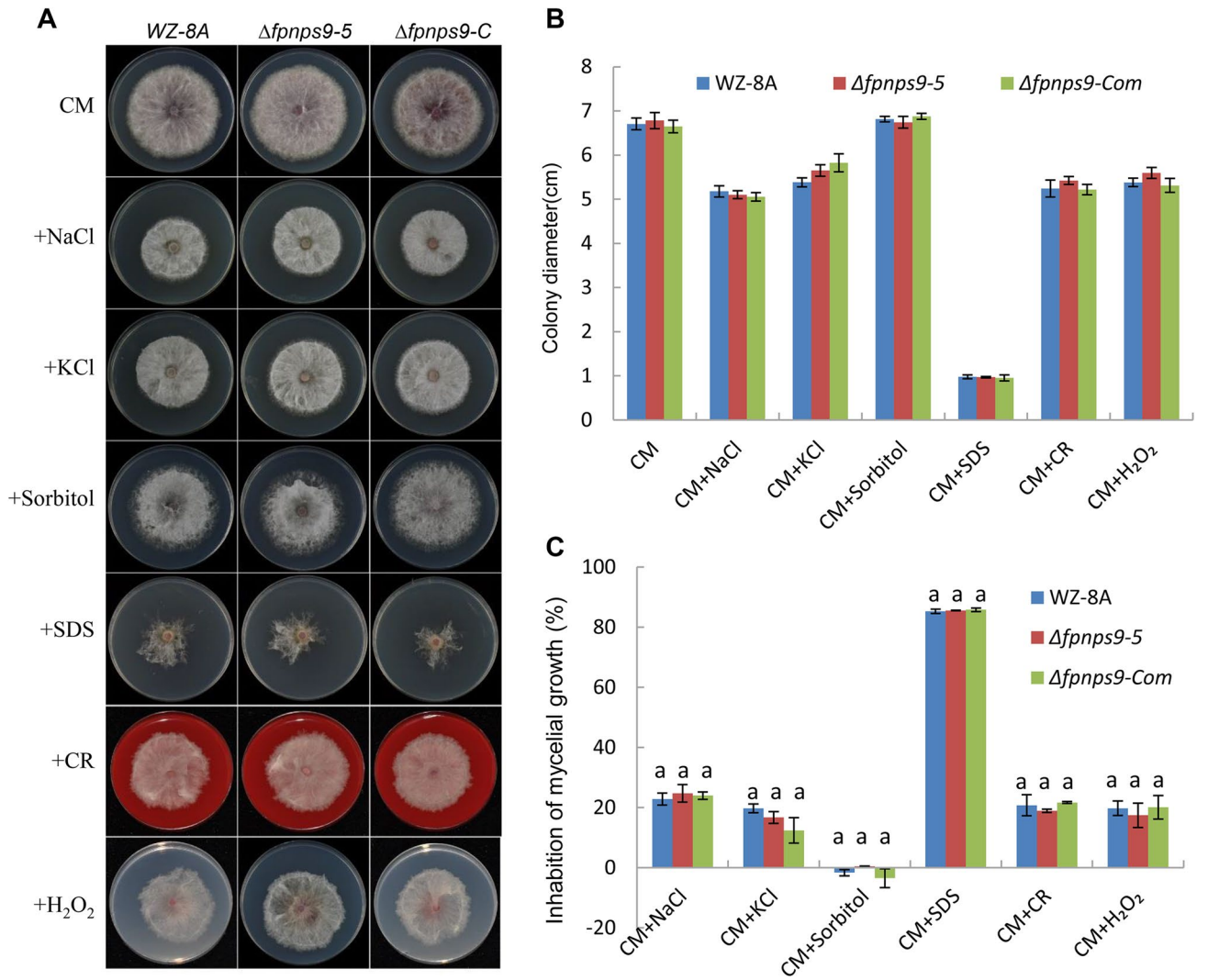

Fig. 5 Sensitivity assays of WT, *Δfpnps9-5*, and *Δfpnps9-C* strains in the presence of different stresses. **a** Colonies of strains on CM medium without and with 1 M NaCl, 1 M KCl, 1 M Sorbitol, 0.05% SDS, 1 mg/ml Congo Red (CR), 20 mM H_2O_2. **b** Colony diameter of each strain was measured 72 h at 25 °C after inoculation on complete agar media without or with additions. Error bars denote the standard deviation of three repeated experiments. **c** Mycelial growth inhibition rate was quantified 72 h at 25 °C after inoculation on CM medium. Strains growing on CM medium without additions were controls. Error bars refer to the standard deviation of three repeated experiments. Same letters indicate no significant difference ($P > 0.05$, Student's *T* test)

not affect morphology, growth rate, and iron absorption when grown on culture media.

Deletion mutant *Δfpnps9* had no defects on several stress conditions

To test the response in stress conditions, we added several common compounds in CM medium induced different stress responses. Under treatments by 1 M NaCl, 1 M KCl, 1 M Sorbitol, 0.05% SDS, 1 mg/ml Congo Red (CR), and 20 mM H_2O_2, we measured and calculated the growth rate, which showed no significant difference among WT strain, *Δfpnps9-5* mutant and Δfpnps9-C strain (Fig. 5a–c).

FpNPS9 is important for pathogenicity and virulence in wheat

To determinate the pathogenicity of *Δfpnps9* null deletion mutants, the conidial suspensions of wild-type and *Δfpnps9* null deletion mutants *Δfpnps9-5* were inoculated on intact and injured coleoptiles. The lesions on wheat coleoptile from the *Δfpnps9* deletion mutant were significantly smaller than that of wild type (Fig. 6a, b). The coleoptile samples

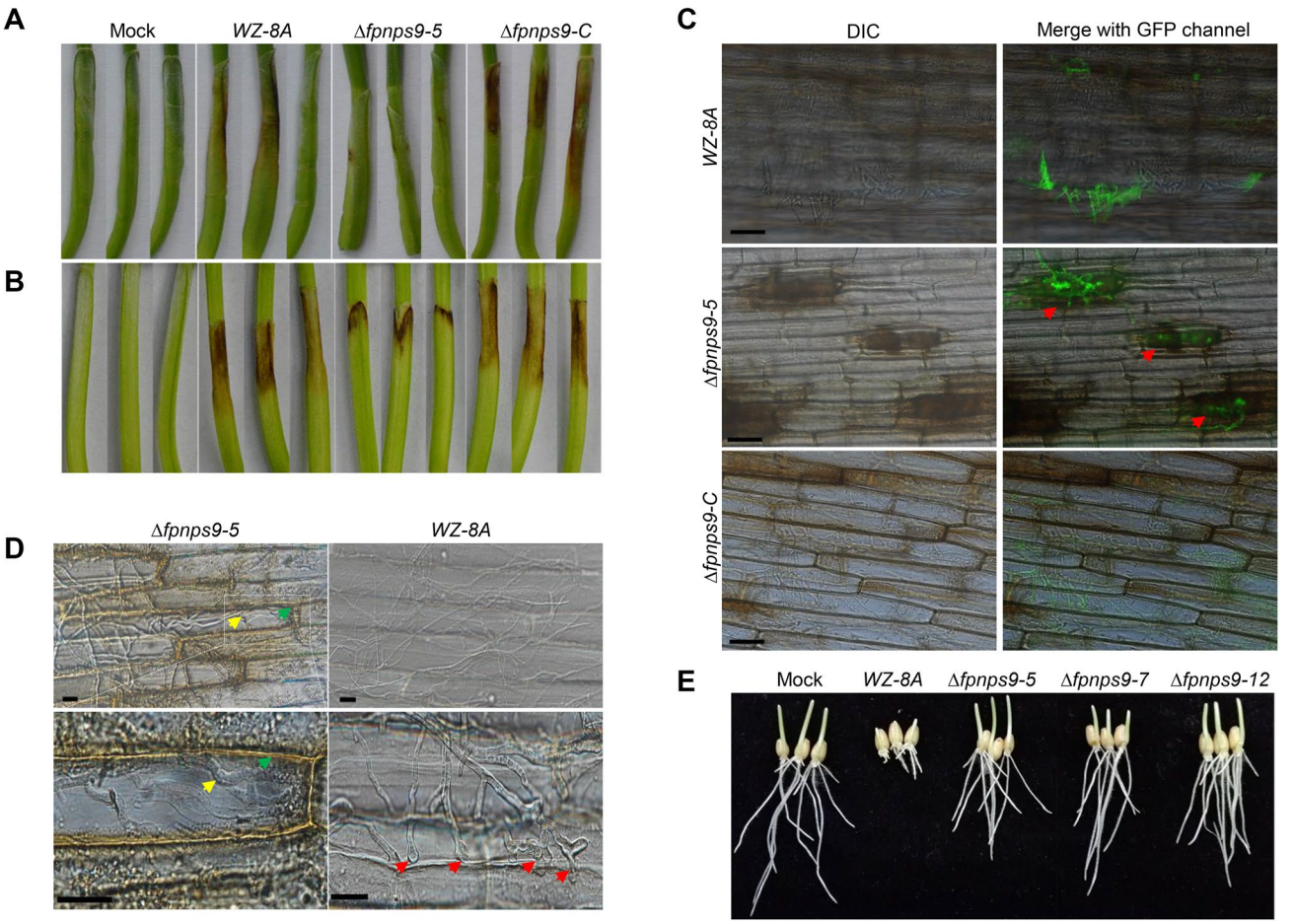

Fig. 6 Pathogenicity assay on susceptible wheat cultivars with the conidial suspension from the *Δfpnps9-5* deletion mutant in comparison with its complemented strain *Δfpnps9*-C and wild-type WZ-8A. **a** Infecting intact wheat coleoptiles with conidial suspension at 1×10^6/ml of WZ-8A, *Δfpnps9-5* and *Δfpnps9-C*. **b** Infecting wounded wheat coleoptiles with conidial suspension at 1×10^7 spores/ml of WZ-8A, *Δfpnps9-5* and *Δfpnps9-C*. Infection were photographed 4 days after inoculation and at least 5 wheat coleoptiles were inoculated. **c** Fluorescent staining by Solophenol Flavine 7GFE for wild-type, mutant*Δfpnps9-5*, and *Δfpnps9-C* when infecting intact wheat coleoptiles. The arrows indicate that hyphae of mutant *Δfpnps9-5* only showed in stomata and not extended to neighbor cells, while WZ-8A and *Δfpnps9-C* had massive infectious hyphae in the wheat coleoptile cells. **d** Histopathology analysis for infection of wounded wheat coleoptiles in comparison with wild-type and *Δfpnps9-5* mutant. The green arrow showed the brownish colorization observed at local cell after infection of *Δfpnps9-5* mutant. The yellow arrows refer to the hyphae of mutant *Δfpnps9-5*. The red arrows showed appressorium-like structure to attempt crossing the cell wall after the infection of wilt type WZ-8A. **e** Inhibition test for wheat germination and growth of radicles and plumules by crude extraction cultured in N-free Czapek medium. CK, N-free Czapek medium only. The scale bars represent 20 μm

were detached to evaluate the biomass on wheat coleoptiles under a fluorescence microscope after staining with fluorescent Solophenol Flavine 7GFE. When inoculated on intact coleoptile, a large amount of mycelia in the tissues of the coleoptile expanded to the surrounding cells and causes large lesion in the wild-type WZ-8A and complemented mutant, while tissues infected with the mutant showed only loose hyphae in stomata, a brownish colorization around the stomata, with limited extension around the lesion, with hyphae unable to reinfect surrounding cells (Fig. 6c). When inoculate on wounded coleoptile, the mutant could invade coleoptile from the injured site, but a brownish colorization around the invasion sites and surrounding cells, the cell wall looked thickened, and the expansion of hyphae is limited, which was absent in tissues infected with the wild type and complemented strain that grew aggressively and lesion formed rapidly (Fig. 6d).

Because NPS is a secondary metabolic gene, DON is an important toxin as well as a kind of secondary metabolite produced by *Fusarium* spp. and as a virulence factor in stem colonization (Mudge et al. 2006). Therefore, we further measured DON production in inoculated wheat grains harvested at 30 dpi. In comparison with wild-type WZ-8A, the Δ*fpnps9* mutant also was significantly reduced in DON production (Table 2).

We further tested the inhibition of elongation of radicles by crudely extracting *Fp* metabolites in PDB, PS and N-free Czapek liquid medium on germinating wheat seeds. The metabolites from wild type and mutant in PDB and PS liquid media had no difference from treatment on wheat seeds, whereas bioactive inhibition was found in N-free Czapek medium. All three *Δfpnps9* deletion mutants exhibited significantly reduced inhibition of radicle growth compared to the wild type (Fig. 6e).

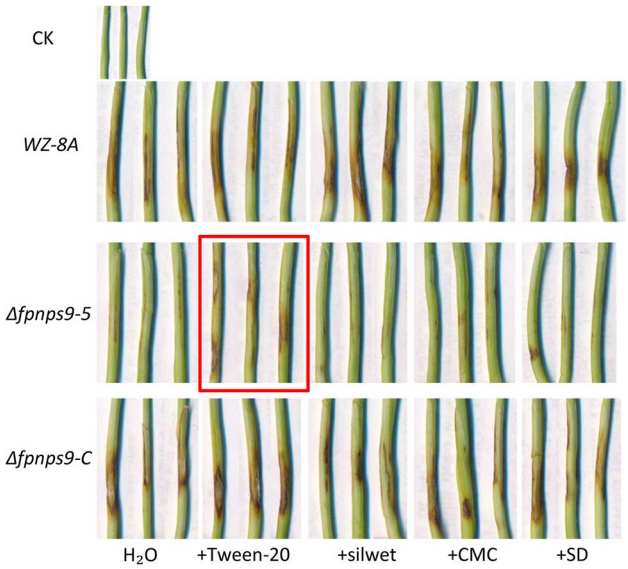

Fig. 8 Pathogenicity assay on intact coleoptiles of susceptible wheat cultivars with the conidial suspension at 0.05% Tween20, silwet, carboxymethyl cellulose (CMC), sodium dodecyl benzene sulfonate (SDBS), and sterile H_2O, respectively. The water with no conidium was monk control. The red box showed the large lesions restored by Tween20

On spikelet inoculation, the wild-type and complemented strains spread out half of wheat head, while the *Δfpnps9* null deletion mutants were confined to the inoculated spikelet still with mycelia growth on the spikelet (Fig. 7). During the pathogenicity test, Tween 20 partially restored the mutant virulence (Fig. S1). We compared four different kinds of surfactants such as silwet, carboxymethyl cellulose (CMC), and sodium dodecyl benzene

Fig. 7 Pathogenicity assay on wheat spikes inoculated with a conidial suspension of each strain and photographed two weeks after inoculation. The arrows showed the inoculation sites

sulfonate (SDBS). Except Tween 20, other surfactants did not increase the severity of lesions (Fig. 8).

Complementation of the *Δfpnps9*, localization of FpNPS9-GFP fusion protein, and the plant-inducted expression of FpNPS9-GFP

To test whether the mutant phenotype could be restored by the wild-type *FpNPS9* gene, a pFpNPS9-GFP fusion construct with a native promoter around 2 kb was transformed into the protoplast of the *Δfpnps9-5* mutant. More than 30 transformants with G418 resistance were obtained. Expression of *FpNPS9* and GFP in FpNPS9-GFP were validated by RT-PCR in the wheat coleoptile infected by wild type and *Δfpnps9*-C with *Δfpnps9-5* mutant as control (Fig. S2). The pathogenicity of the complementary strain *Δfpnps9*-C recovered the reduced pathogenicity on wheat coleoptiles (Fig. 6a–c). No green fluorescence signal was observed in conidia, germ tube, and mycelia of the *Δfpnps9*-C from culture medium (Fig. 9a, b). During infection of wheat coleoptile by *Δfpnps9*-C, the inner epidermis of coleoptile was detached and a strong green fluorescence signal was observed in the germinating conidia, hyphae, and infectious hyphae in or outside of host cells (Fig. 9c).

Discussion

In this study, we cloned and characterized the NPS-like gene *FpNPS9*, the ortholog of *NPS9* in *Fg*. The expression of *FpNPS9* could not be detected using the cDNA from conidia and mycelia in vitro, but could be detected in the infected wheat tissues. In accordance, a strong GFP signal was also observed in the conidia and mycelia in the germinating stage on epidermis cells of coleoptiles. Seong et al. (2008) and Zhang et al. (2012) reported that the expression of NPS9 in *Fg* was consistent and low in vegetative hyphae, a similar pattern as with *FpNPS9*. In *Magnaporthe oryzae*, *ACE1* encodes a cytoplasmic fusion polypeptide containing a polyketide synthase (PKS) and a nonribosomal peptide synthetase (NRPS) and is exclusively expressed in appressoria without special signals from host. Deletion of *ACE1* did not significantly compromise virulence, but Ace1-mediated biosynthetic activity as the fungal effector is required for avirulence in Pi33 resistant rice cultivar, although this kind

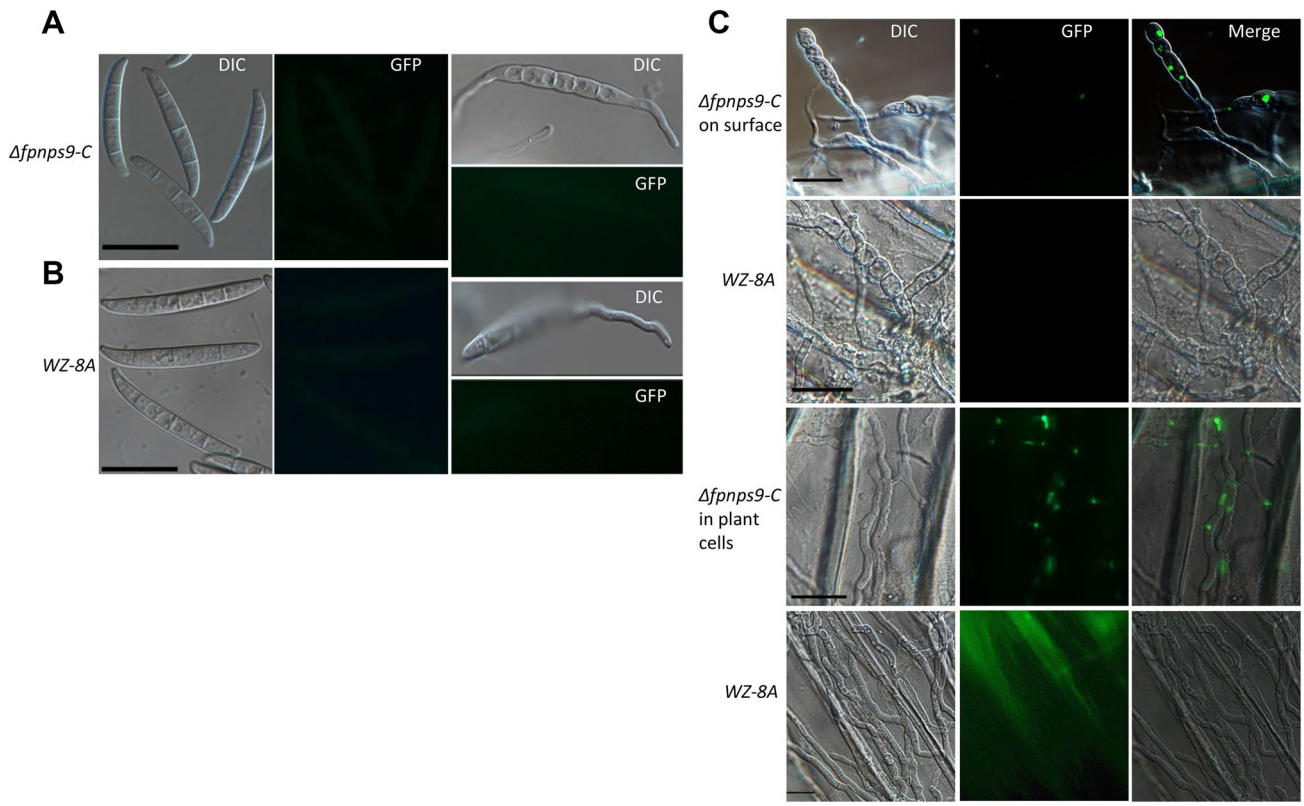

Fig. 9 Subcellular localization of FpNPS9-GFP in *Δfpnps9-C* after the infection of wheat coleoptiles at 36 h was photographed using a Nikon ECLIPSE microscope at 488 nm excitation and 530 nm emission wavelengths. **a**, **b** Conidium and germ tube in culture media. **c** Germinating conidium on the surface of host cells and infectious hyphae in coleoptile cells of wheat infection. *DIC,* differential interference contrast; *GFP,* green fluorescent channel. The scale bar = 20μm

of avirulent effector may not be secreted. Ace1 indirectly mediates recognition of Pi33 (Bohnert et al. 2004; Collemare et al. 2010; Fudal et al.,2007; Song et al. 2015). In *Fp*, *FpNPS9* has the similar expression pattern with *ACE1* in rice infection. Determining the host inducible substances potentially interacting with the product of *FpNPS9* should be the focus of further research.

No obvious difference on the morphology, growth rate on PDA and -Fe Czapek medium, and conidiation in CMC medium was found compared to wild type with the exception of the hyphal tip. A tolerance assay to several compounds of the *Δfpnps9-5* mutant exhibited no differences from the wild-type strain and complemented strain. The *Δnps9* in *Fg* also did not showed detectable defects in radial growth, colony, and conidial morphology in vitro when treated on all the tested culture conditions (Jia et al. 2019). The only difference between *Δfpnps9-5* and *Δnps9* is the hyphae tip morphology. The deletion of *FpNPS9* affected the morphology of vegetative hyphae, but radial growth was normal. Secondary metabolism (SM) plays an important role in the metabolism of organisms. Recent studies have shown that *NPS* genes are associated with pathogenicity of fungi, such as *C. fulvum* (Collemare et al. 2014), *A. alternata* (Johnson et al. 2000), *C. heterostrophus* (Lee et al. 2005), *C. miyabeanus*, and *A. brassicicola* (Oide et al. 2006). *NPS1*, *NPS2*, *NPS6* (Oide et al. 2006, 2014), and *NPS9* (Zhang et al. 2012) have been reported to be associated with pathogenicity in *Fg*. Mudge et al. (2006) reported that DON production contributed to stem colonization in *Fg* and *Fp*. Deletion of *FpNPS9* led to significant reduction of DON synthesis and pathogenicity during wheat coleoptiles infection, indicating that the *FpNPS9* was responsible for pathogenicity. Histopathological examination under the microscope showed that hyphae were restricted in the local infection site and could not extend in the mutant, along with a brownish pigment accumulated around the infection sites of infection and the cell wall looks thickened. This may be due to the *Δfpnps9-5* mutant lost the ability to extend or to break through the host's defense. The brownish colorization triggered maybe because the lignin accumulation or hypersensitive response in cells around infection sites. We found Tween 20 as surfactant could change the infection result of mutant. The similar result was observed in the repeated experiments. Generally, Tween 20 is a polyoxyethylene sorbitol ester, containing 20 ethylene oxide units, 1 sorbitol, and 1 lauric acid as the primary fatty acid. It was speculated that Tween 20 might be similar to the *FpNPS9* gene product or intermediate which was required for infection of wheat. The *Fg3-54* cluster including NPS9 and NPS5 in *Fg* contributes linear fusaoctaxin A production. Fusaoctaxin A as a virulence factor suppresses tissue specific gene expressing in the chloroplast and/or plasmodesmata (Jia et al. 2019). In contrast, the *Δfpnps9-5* mutant with abnormal hyphal tip caused not only the thicker cell wall in the inoculated cell, but triggered local host cell with strong brown to dark brown pigmentation in compare with wild-type and complemented strain indicating *FpNPS9* may involve in suppressing host defensing response to facilitate the fungal infection. The exogenous Fusaoctaxin A suppressed classes of gene expression in defense response by callose deposition. The *Fg3-54* cluster is similar to that in *Fp* and FpNps9 was composed of similar domains with Nps9. Whether the product of *FpNPS9* involving in Fusaoctaxin A or other nonribosomal peptide needs to be determinate in the future study.

The deletion of *FpNPS9* gene in *F. pseudograminearum* caused the reduced DON production and pathogenicity. The inhibition of root elongation was significant reduced. The *Δfpnps9-5* mutant also was not able to spread into other spikelet, it was confined to the inoculated spikelet, which is in accordance with the tri5 disruption mutant in *Fg* (Maier et al. 2006). DON might be important virulence factor in *Fp* extension of coleoptiles and spikes. Our previous results in a potted infection assay where the elongation of roots and aboveground part of seedlings were seriously inhibited (Yong-Hui et al. 2017). The similar phenomenon of DON inhibition on germinating seeds and root elongation of wheat was reported by Rocha et al. (2005).

Based on previous studies, we tried to extract the toxin by shaking the culture of *fpnps9-5* and WT in PS and PDB liquid media. But inhibition assays of wheat radicle and germ were not different between wild type and mutant. We tried to culture with boiled malt juice and wheat seedling juice (filtered fresh wort by bacterial filtration) to induce gene expression, however, there was no significant difference between wild type and mutant. The culture medium with low nutrition or nitrogen-free can partially induce some toxin-related gene expression (Guldener et al. 2006; Ilgen et al. 2009), therefore, we used modified Czapek and nitrogen-free Czapek culture media to test the bioactivity of metabolite, and found the mutants were shown reduced inhibition of seedlings compared to the wild type. These means that *FpNPS9* gene might participate in toxin production and metabolism on certain conditions.

In summary, we characterized the *FpNPS9* function in *F. pseudograminearum* for the first time. The *Δfpnps9* is not changed in growth, conidiation, and common stresses except the hyphae tip morphology. *FpNPS9* is specifically induced during plant infection, and plays pleiotropic roles in DON production, pathogenicity and extension in wheat. Our findings would be benefit for the understanding of secondary metabolism and pathogenicity in *F. pseudograminearum* and other filamentous phytopathogens. The uncovering interaction of *FpNPS9* product and wheat inducers should promote the wheat breeding for resistance to Fusarium crown rot disease.

Acknowledgements We give thanks to Dr. Daniel Ebbole (Texas A&M University, College Station, TX, USA) for a critical reading of the manuscript. This work was supported by National Key R&D Program of China (Grant number 2017YFD0301104) and National Special Fund for Agro-scientific Research in the Public Interest (Grant number 201503112).

References

Akinsanmi OA et al (2004) Identity and pathogenicity of Fusarium spp. isolated from wheat fields in Queensland and northern New South Wales. Aust J Agric Res 55:97–107. https://doi.org/10.1071/ar03090

Akinsanmi OA et al (2006) Genetic diversity of Australian *Fusarium graminearum* and *F.pseudograminearum*. Plant Pathol 55:494–504. https://doi.org/10.1111/j.1365-3059.2006.01398.x

Bohnert HU et al (2004) A putative polyketide synthase/peptide synthetase from *Magnaporthe grisea* signals pathogen attack to resistant rice. Plant Cell 16:2499–2513. https://doi.org/10.1105/tpc.104.022715

Collemare J, Pianfetti M, Houlle AE, Morin D, Camborde L, Gagey MJ et al (2010) *Magnaporthe grisea* avirulence gene ace1 belongs to an infection-specific gene cluster involved in secondary metabolism. New Phytol 179(1):196–208. https://doi.org/10.1111/j.1469-8137.2008.02459.x

Collemare J et al (2014) Secondary metabolism and biotrophic lifestyle in the tomato pathogen *Cladosporium fulvum*. PLoS ONE 9:e85877. https://doi.org/10.1371/journal.pone.0085877

Ding M, Li J, Fan X, He F, Yu X, Chen L et al (2018) Aquaporin1 regulates development, secondary metabolism and stress responses in *Fusarium graminearum*. Curr Genet 64:1057. https://doi.org/10.1007/s00294-018-0818-8

Dyer AT, Johnston RH, Hogg AC, Johnston JA (2009) Comparison of pathogenicity of the fusarium crown rot (fcr) complex (*F. culmorum*, *F. pseudograminearum* and *F. graminearum*) on hard red spring and durum wheat. Eur J Plant Pathol 125(3):387–395

Fudal I, Collemare J, Bohnert HU, Melayah D, Lebrun MH (2007) Expression of *Magnaporthe grisea* avirulence gene ace1 is connected to the initiation of appressorium-mediated penetration. Eukaryot Cell 6(3):546–554. https://doi.org/10.1128/EC.00330-05

Guldener U et al (2006) Development of a *Fusarium graminearum* Affymetrix GeneChip for profiling fungal gene expression in vitro and in planta. Fungal Genet Biol 43:316–325. https://doi.org/10.1016/j.fgb.2006.01.005

Hansen FT et al (2012) Overexpression of NRPS4 leads to increased surface hydrophobicity in *Fusarium graminearum*. Fungal Biol 116:855–862. https://doi.org/10.1016/j.funbio.2012.04.014

Hansen FT et al (2015) An update to polyketide synthase and non-ribosomal synthetase genes and nomenclature in Fusarium. Fungal Genet Biol 75:20–29. https://doi.org/10.1016/j.fgb.2014.12.004

He X (2016) Genetic diversity and pathogenicity analysis of *Fusarium pseudograminearum* that is the dominant pathogen causing crown rot of wheat Henan Agricultural Univeristy. Master thesis

Ilgen P, Hadeler B, Maier FJSW (2009) Developing kernel and rachis node induce the trichothecene pathway of *Fusarium graminearum* during wheat head infection. Mol Plant Microb Interact 22(8):899–908. https://doi.org/10.1094/MPMI-22-8-0899

Jia Lei-Jie, Tang Hao-yu, Wang Wan-qiu, Yuan Ting-lu et al (2019) A linear nonribosomal octapeptide from *Fusarium graminearum* facilitates cell-to-cell invasion of wheat. Nat Commun 10:922. https://doi.org/10.1038/s41467-019-08726-9

Johnson RDJL, Itoh Y et al (2000) Cloning and characterization of acyclic peptide synthetase gene from *Alternaria alternata* apple pathotype whose product is involved in AM-toxin synthesis and pathogenicity. Mol Plant Microbe Interact 13:742–753. https://doi.org/10.1094/mpmi.2000.13.7.742

Kazan K, Gardiner DM (2018) Fusarium crown rot caused by *Fusarium pseudograminearum* in cereal crops: recent progress and future prospects. Mol Plant Pathol 19:1547–1562. https://doi.org/10.1111/mpp.12639

Knight N, Sutherland M (2011) A rapid differential staining technique for *Fusarium pseudograminearum* in cereal tissues during crown rot infections. Plant Pathol 60(6):1140–1143. https://doi.org/10.1111/j.1365-3059.2011.02462.x

Knight N, Sutherland M (2013) Histopathological assessment of wheat seedling tissues infected by *Fusarium pseudograminearum*. Plant Pathol 62(3):679–687. https://doi.org/10.1111/j.1365-3059.2012.02663.x

Lee BN et al (2005) Functional analysis of all nonribosomal peptide synthetases in *Cochliobolus heterostrophus* reveals a factor, NPS6, involved in virulence and resistance to oxidative stress. Eukaryot Cell 4:545–555. https://doi.org/10.1128/EC.4.3.545-555.2005

Leslie JF, Summerell BA (2006) The Fusarium laboratory manual. Chapter 7, Nucleic Acid Analyses, p57-63. Blackwell Publishing Professional 2121 State Avenue, Ames, Iowa 50014, USA. SB741. F9L47 2006, 632′.4677-dc22, 2006004759

Li HL et al (2012) First report of *Fusarium pseudograminearum* causing crown rot of wheat in Hena, China. Plant Dis 96:1065. https://doi.org/10.1094/PDIS-01-12-0007-PDN

Liu C, Ogbonnaya FC (2015) Resistance to Fusarium crown rot in wheat and barley: a review. Plant Breed 134:365–372. https://doi.org/10.1111/pbr.12274

Maier FJ, Miedaner T, Hadeler B, Felk A, Salomon S, Lemmens M et al (2006) Involvement of trichothecenes in fusarioses of wheat, barley and maize evaluated by gene disruption of the trichodiene synthase (tri5) gene in three field isolates of different chemotype and virulence. Mol Plant Pathol 7(6):449–461. https://doi.org/10.1111/j.1364-3703.2006.00351.x

Malligan CD (2009) Crown rot (*Fusarium pseudograminearum*) symptom development and pathogen spread in wheat genotypes with varying disease resistance. Ph.D. thesis

Mudge AM, Dillmacky R, Dong Y, Gardiner DM, White R, Manners JM (2006) A role for the mycotoxin deoxynivalenol in stem colonisation during crown rot disease of wheat caused by *Fusarium graminearum* and *Fusarium pseudograminearum*. Physiol Mol Plant Pathol 69(1):73–85. https://doi.org/10.1016/j.pmpp.2007.01.003

Murray GM, Brennan JP (2009) Estimating disease losses to the Australian wheat industry. Austr Plant Pathol 38:558–570

Obanor F, Chakraborty S (2014) Aetiology and toxigenicity of *Fusarium graminearum* and *F. pseudograminearum* causing crown rot and head blight in Australia under natural and artificial infection. Plant Pathol 63:1218–1229. https://doi.org/10.1111/ppa.12200

Oide S et al (2006) NPS6, encoding a nonribosomal peptide synthetase involved in siderophore-mediated iron metabolism, is a conserved virulence determinant of plant pathogenic ascomycetes. Plant Cell 18:2836–2853. https://doi.org/10.1105/tpc.106.045633

Oide S et al (2007) Intracellular siderophores are essential for ascomycete sexual development in heterothallic *Cochliobolus heterostrophus* and homothallic *Gibberella zeae*. Eukaryot Cell 6:1339–1353. https://doi.org/10.1128/EC.00111-07

Oide S et al (2014) Individual and combined roles of malonichrome, ferricrocin, and TAFC siderophores in *Fusarium graminearum* pathogenic and sexual development. Front Microbiol 5:759. https://doi.org/10.3389/fmicb.2014.00759

Powell JJ et al (2017) The Fusarium crown rot pathogen *Fusarium pseudograminearum* triggers a suite of transcriptional and metabolic changes in bread wheat (*Triticum aestivum* L.). Ann Bot. https://doi.org/10.1093/aob/mcw207

Rocha O, Ansari K, Doohan FM (2005) Effects of trichothecene mycotoxins on eukaryotic cells: a review. Food Addit Contam 22(4):369–378. https://doi.org/10.1080/02652030500058403

Romans-Fuertes P et al (2016) Identification of the non-ribosomal peptide synthetase responsible for biosynthesis of the potential anti-cancer drug sansalvamide in *Fusarium solani*. Curr Genet 62:799–807. https://doi.org/10.1007/s00294-016-0584-4

Seong KY et al (2008) Conidial germination in the filamentous fungus *Fusarium graminearum*. Fungal Genet Biol Fg B 45:389–399. https://doi.org/10.1016/j.fgb.2007.09.002

Singh RP et al (2016) Disease impact on wheat yield potential and prospects of genetic control. Annu Rev Phytopathol 54:303–322. https://doi.org/10.1146/annurev-phyto-080615-095835

Smiley RW et al (2005) Crop damage estimates for crown rot of wheat and barley in the Pacific Northwest. Plant Dis 89:595–604. https://doi.org/10.1094/PD-89-0595

Song Z, Bakeer W, Marshall JW, Yakasai AA, Khalid RM, Collemare J et al (2015) Heterologous expression of the avirulence gene ace1 from the fungal rice pathogen *Magnaporthe oryza*e. Chem Sci 6(8):4837–4845. https://doi.org/10.1039/c4sc03707c

Sørensen JL et al (2018) The cereal pathogen *Fusarium pseuodograminearum* produces a new class of active cytokinins during infection. Mol Plant Pathol. https://doi.org/10.1111/mpp.12593

Sun BJ et al (2015) Establishment of SYBR Green I Real-Time PCR for quantitatively detecting *Rhizoctonia cerealis* in winter wheat. Sci Agric Sin. https://doi.org/10.3864/j.issn.0578-1752.2015.01.0

Tobiasen C et al (2007) Nonribosomal peptide synthetase (NPS) genes in *Fusarium graminearum*, *F. culmorum* and *F. pseudograminearium* and identification of NPS2 as the producer of ferricrocin. Curr Genet 51:43–58. https://doi.org/10.1007/s00294-006-0103-0

Wang LM et al (2017) FpPDE1 function of *Fusarium pseudograminearum* on pathogenesis in wheat. J Integr Agric 16:2504–2512. https://doi.org/10.1016/S2095-3119(17)61689-7

Xu F et al (2015) First report of *Fusarium pseudograminearum* from wheat heads with fusarium head blight in North China Plain. Plant Dis 99:156. https://doi.org/10.1094/PDIS-05-14-0543-PDN

Yang P, Chen Y, Wu H et al (2018) The 5-oxoprolinase is required for conidiation, sexual reproduction, virulence and deoxynivalenol production of *Fusarium graminearum*. Curr Genet 64:285. https://doi.org/10.1007/s00294-017-0747-y

Yong-Hui LI et al (2017) Differential expression of three plant hormone related genes in wheat infected by *Fusarium pseudograminearum*. Acta Agronomica Sinica 43:1632. https://doi.org/10.3724/SP.J.1006.2017.01632

Zhang XW et al (2012) In planta stage-specific fungal gene profiling elucidates the molecular strategies of *Fusarium graminearum* growing inside wheat coleoptiles. Plant Cell 24:5159–5176. https://doi.org/10.1105/tpc.112.105957

Zhou H, He X, Wang S, Ma Q, Sun B, Ding S et al (2019) Diversity of the Fusarium pathogens associated with crown rot in the Huanghuai wheat growing region of china. Environ Microbiol 15:20. https://doi.org/10.1111/1462-2920.14602